



# Incorporation of Zero-Valent Silver and Polyvinyl Acetate on the Surface Matrix of Carbon Nanotubes for the Adsorption of Mercury and Chromium from Industrial Wastewater

T. C. Egbosiuba<sup>1,\*</sup>

<sup>1</sup> Chemical Engineering Department, Chukwuemeka Odumegwu Ojukwu University, Uli Campus, Anambra State, NIGERIA

## Abstract

Herein, zero-valent silver ( $\text{Ag}^0$ ) and polyvinyl acetate (PVAc) was ultrasonically incorporated into the surface matrix of MWCNTs to produce a multifunctional MWCNTs- $\text{Ag}^0$ /PVAc nanocomposite. The MWCNTs, MWCNTs- $\text{Ag}^0$  and MWCNTs- $\text{Ag}^0$ /PVAc were characterized for the thermal stability, crystallographic structure and morphology using thermogravimetric analysis (TGA), X-ray diffraction (XRD) and high resolution scanning electron microscopy (HRSEM). Industrial wastewater containing Hg(II) and Cr(VI) ions were treated using the fabricated MWCNTs- $\text{Ag}^0$ /PVAc at different adsorption parameters such as pH, adsorbent mass, adsorption time and temperature. The characterization result obtained indicated successful incorporation of the  $\text{Ag}^0$  and PVAc to the surface matrix of MWCNTs- $\text{Ag}^0$ /PVAc. The materials were thermally stable and the crystalline peaks/patterns of the incorporated materials were evident on the MWCNTs- $\text{Ag}^0$ /PVAc. The adsorption study revealed maximum adsorption capacity of 249 mg/g and 237 mg/g for the Hg(II) and Cr(VI) by MWCNTs- $\text{Ag}^0$ /PVAc at the pH (6 for Hg(II) and 3 for Cr(VI)), adsorbent mass (40 mg), adsorption time (60 min) and temperature (30 °C). The experimental data effectively fitted the Langmuir isotherm and pseudo-second order kinetic, respectively. Finally, MWCNTs- $\text{Ag}^0$ /PVAc showed remarkable performance as a suitable adsorbent for heavy metals removal from industrial wastewater.

**Keywords:** Multi-walled carbon nanotubes, zero-valent silver, polyvinyl acetate, mercury, chromium, wastewater, adsorption.

## 1.0 INTRODUCTION

In the field of environmental sciences, pollution of water resources due to the anthropogenic activities in the industries had generated a global water crisis. Heavy metals constitute bulk of the pollutants contained in industrial effluents threatening the ecosystem and human health [1]. Among the cationic and anionic heavy metal ions, mercury (II) ( $\text{Hg}^{2+}$ ) and chromium (VI) ( $\text{Cr}^{6+}$ ) had attracted substantial global concern and interest to researchers due to their prevalence in the wastewater as  $\text{HCrO}_4^-$ ,  $\text{H}_2\text{CrO}_4$ ,  $\text{Cr}_2\text{O}_7^{2-}$ ,  $\text{Cr}_3\text{O}^{10-}$  and  $\text{Cr}_4\text{O}^{13-}$  which are basically known to be non-degradable, highly toxic and very mobile [1]. Generally, mercury are released to the environment from industrial activities such as pharmaceuticals, paint production, non-ferrous smelting, waste incineration, production of pesticides and electrical

production [2,3], while chromium are released from battery, leather, electroplating, cosmetics, tanning, textiles and plastic industries [4,5]. The accumulation of mercury in the human body causes severe damages to the skin, liver, kidney, thyroid, immune system and central nervous system [2]. Also, prolonged exposure to chromium are carcinogenic, mutagenic, causes diarrhea, asthma and severe damage to the brain, kidney and liver [4,6]. Therefore, it is a pressing task to remove mercury and chromium from wastewater to be in the recommended concentration of drinking water range from 0.002 to 0.006 mg/L and 0.06 to 0.09 mg/L [7].

Before now, a number of treatment methods have been applied for the treatment of wastewater such as adsorption, coagulation-flocculation, ion exchange, filtration, photocatalysis, membrane separation, chemical precipitation, floatation and evaporation [8–13]. Nevertheless, few of these techniques are suitable for heavy metal removal application due to disadvantages such as high cost of production, low efficiency of purification, generation of large quantity of waste and complex operations [14–16]. Of these, adsorption

\*Corresponding author (Tel: +234 (0) 8033239501)

Email addresses: [ct.egbosiuba@coou.edu.ng](mailto:ct.egbosiuba@coou.edu.ng) (T. C. Egbosiuba)

technique presents excellent wastewater treatment potential and predominantly used due to its high removal efficiency, low-cost, environmental friendliness, easy handling and highly effective adsorbents [17,18]. A good number of adsorbents such as agricultural waste, biochar, activated carbon, clay, zeolite, graphene, carbon nanotubes, chitosan, metal nanoparticles, metal organic frameworks and composites of materials have been employed to treat heavy metals contaminated wastewater [19–23]. In the past, studies have been carried out using multi-walled carbon nanotubes (MWCNTs) to remove heavy metal ions from wastewater [15,16,24].

Previous research have also reported the incorporation of materials such as silver nanoparticles, nickel nanoparticles, chitosan, polyethylene glycol and graphene oxide into the surface matrix of MWCNTs for effective adsorption of heavy metals [25,26]. To the best of our knowledge, no study have investigated the incorporation of polyvinyl acetate on the surface matrix of MWCNTs for the removal of Hg(II) and Cr(VI) ions from wastewater.

In this study, silver nanoparticles ( $\text{Ag}^0$ ) and PVAc was incorporated into the surface matrix of MWCNTs. The obtained MWCNTs, MWCNTs- $\text{Ag}^0$  and MWCNTs- $\text{Ag}^0/\text{PVAc}$  were characterized using thermogravimetric analysis (TGA), X-ray diffraction (XRD) and high resolution scanning electron microscopy (HRSEM) to ascertain the thermal stability, crystalline structure and morphology. Further investigation of the adsorption capacity of MWCNTs- $\text{Ag}^0/\text{PVAc}$  towards Hg(II) and Cr(VI) was conducted at different pH, adsorbent mass, adsorption time and temperature. The experimental data from the adsorption studies were subjected to isotherm models and kinetic models to determine the mechanism of the process. The thermodynamic parameters were also determined for the effectiveness of Hg(II) and Cr(VI) adsorption by MWCNTs- $\text{Ag}^0/\text{PVAc}$ .

## 2.0 MATERIALS AND METHODS

### 2.1 Materials

The chemicals such as polyvinyl acetate (PVAc), sodium hydroxide (NaOH), sulphuric acid ( $\text{H}_2\text{SO}_4$ ), nitric acid ( $\text{HNO}_3$ ) and ethanol were in the purity range of 98 to 99.5% and purchased from Sigma Aldrich, Lagos. All the chemicals utilized in this study were of analytical grade and used as received without further purification. The entire solution preparation was carried out using deionized water. The industrial wastewater was obtained from industrial layout, Nnewi Anambra State. The MWCNTs and zero valent silver ( $\text{Ag}^0$ ) used in this study were prepared as reported elsewhere [5,16,27].

### 2.2 Preparation MWCNTs- $\text{Ag}^0/\text{PVAc}$

Initially, the MWCNTs was purified and oxidized by ultrasonication technique using the procedure reported elsewhere [16,17]. Particularly, 10 g of MWCNTs was mixed into 250 mL Erlenmeyer flask containing a solution of  $\text{H}_2\text{SO}_4$  (10 mL) and  $\text{HNO}_3$  (30 mL) placed in an ultrasonic bath at 60 °C for 3 h. Thereafter, the oxidized MWCNTs was washed to a pH around 7 using distilled water and oven dried overnight at 100 °C. Subsequently, 5 g of  $\text{Ag}^0$  was added to a 2.5 g of PVAc dissolved in a 200 mL mixed solution of ethanol and water (ratio 1:1, v/v) under continuous sonication at 40 °C for 2 h. Then, the oxidized MWCNTs was added to the mixture and the sonication continued for another 1 h. Afterwards, the mixture was filtered using Whatman No. 1 filter paper prior to oven drying at 105 °C for 10 h. The adsorbent obtained was stored in a safe bottle labelled MWCNTs- $\text{Ag}^0/\text{PVAc}$  until further use.

### 2.3 Characterization of Materials

The MWCNTs, MWCNTs- $\text{Ag}^0$  and MWCNTs- $\text{Ag}^0/\text{PVAc}$  were characterized for thermal stability, crystallographic and morphological structure. Thermal stability investigation of the samples was determined using thermogravimetric analysis (TGA, PerkinElmer, UK) using temperature increase of 10 °C/min under nitrogen environment. A diffractometer (XRD, 6000, Shimadzu Scientific) was used to conduct the XRD analysis on the adsorbent to evaluate the crystallinity and phase structures. Also, scanning electron microscopy (SEM) was used to determine the morphological representations of the MWCNTs and MWCNTs- $\text{Ag}^0/\text{PVAc}$ . The surface properties of the MWCNTs- $\text{Ag}^0/\text{PVAc}$  were performed using Brunauer–Emmett–Teller (BET, NOVA 4200, UK) technique.

### 2.4 Adsorption Tests

The evaluation of adsorption capacity of MWCNTs- $\text{Ag}^0/\text{PVAc}$  towards Cr(VI) and Hg(II) at initial concentrations ( $C_0$ ) of 50 mg/L were conducted in a batch mode at various process parameters such as pH, adsorption time, adsorbent mass and temperature. Initially, the influence of pH on the removal of the metal ions was investigated in the pH range 1 – 7 by adding 15 mg of MWCNTs- $\text{Ag}^0/\text{PVAc}$  into a 200 mL conical flask containing 50 mL of Cr(VI) and Hg(II) ions solution in a water bath at constant adsorption time and temperature of 30 min and 30 °C, respectively. To investigate the adsorption time influence on the removal of Cr(VI) and Hg(II) ions by MWCNTs- $\text{Ag}^0/\text{PVAc}$ , 15 mg of the adsorbent was added to the 50 mL of the wastewater solution maintained at pH (6 for Hg(II) and 3 for Cr(VI))

in a corked 200 mL conical flask and placed in a water bath at 30 °C for the various adsorption time of 20, 30, 40, 50, 60 and 90 min, respectively. The influence of adsorbent mass on the removal of Cr(VI) and Hg(II) was examined at constant pH (6 for Hg(II) and 3 for Cr(VI)), adsorption time (60 min) and temperature (30 °C) by adding different MWCNTs-Ag<sup>0</sup>/PVAc mass of 5, 10, 15, 20, 25 and 30 mg into a 50 mL wastewater contained in a 200 mL conical flask placed in a water bath. For the temperature influence of the removal of Cr(VI) and Hg(II) ions from wastewater, 30 mg of MWCNTs-Ag<sup>0</sup>/PVAc was added to 250 mL conical flask containing the wastewater at pH (6 for Hg(II) and 3 for Cr(VI)) in a water bath for 60 min at 30, 35, 40, 45, 50, 55 and 60 °C, respectively. At the end of each pH, adsorption time, adsorbent mass and temperature variation, the mixture was filtered using Whatman No. 1 filter paper and the filtrate analyzed for the residual concentrations of Cr(VI) and Hg(II) using atomic adsorption spectrometry (AAS, PG 990, PG Instruments, UK) technique. The adsorption capacity ( $q_e$ , mg/g) at equilibrium and the removal percentage (R%) of the metal ions were evaluated using Eqs. (1) and (2) [28,29].

$$q_e = \frac{(C_0 - C_e) \times V}{m} \quad (1)$$

$$R\% = \frac{C_0 - C_{e,t}}{C_0} \times 100\% \quad (2)$$

In which  $C_0$  (mg/L) refers to the initial concentration of Cr(VI) and Hg(II) ions, while  $C_e$  (mg/L) represent the equilibrium concentrations of Cr(VI) and Hg(II) ions. Also,  $m$  (mg) and  $V$  (L) indicate the used mass of MWCNTs-Ag<sup>0</sup>/PVAc and the adsorbate solution volume.

### 3.0 RESULTS AND DISCUSSION

#### 3.1 Characterization of materials

The MWCNTs, MWCNTs-Ag<sup>0</sup> and MWCNTs-Ag<sup>0</sup>/PVAc were subjected to thermogravimetric analysis to determine their thermal stability and the results of the thermogram presented in Figure 1a. The thermogram curve for the MWCNT, MWCNTs-Ag<sup>0</sup> and MWCNTs-Ag<sup>0</sup>/PVAc showed similar pattern but differs slightly in their thermal stability. The thermogram curve of the MWCNTs did not show initial weight loss to moisture but was stable up to the temperature of 300 °C, while MWCNTs-Ag<sup>0</sup> and MWCNTs-Ag<sup>0</sup>/PVAc revealed noticeable degradation which were attributed to the loss of moisture. As shown by the thermogram, the peak decomposition temperature and percentage weight loss observed on the MWCNTs were 450 °C and 55%,

respectively. The thermogram curve of MWCNT-Ag<sup>0</sup> exhibited peak decomposition temperature at 442 °C and percentage weight loss of 78%. At the temperature of 439 °C, the maximum percentage weight loss of 92% was recorded for MWCNTs-Ag<sup>0</sup>/PVAc. As seen from the TGA results, MWCNTs exhibited better thermal stability followed by MWCNTs-Ag<sup>0</sup> and MWCNTs-Ag<sup>0</sup>/PVAc. The observed trend in the thermal stability of the materials may be attributed to the incorporation of Ag<sup>0</sup> and PVAc to the surface matrix of MWCNTs.

The phase structure of MWCNTs, MWCNTs-Ag<sup>0</sup> and MWCNTs-Ag<sup>0</sup>/PVAc were examined using XRD technique and the spectrum obtained shown in Figure 1b. The result shows the samples were predominantly composed of carbon and the XRD spectra of MWCNTs demonstrated intense, sharp and strong peaks at the 2 theta values of 26.6°, 44.4°, 51.2°, 75.2° and 77.5° which were assigned to the crystal planes of (002), (101), (102), (200) and (204), respectively. Also, the evaluated average crystallite sizes of 6.80 nm were obtained for the MWCNTs using Debye-Scherrer equation. Correspondingly, the XRD pattern of MWCNTs-Ag<sup>0</sup> revealed the presence of graphite carbon with diffraction peaks at the 2 theta values of 26.6°, 44.4° and 77.5° that corresponds to the crystal planes of (002), (101) and (204). The diffraction peaks of Ag<sup>0</sup> were observed at 38.1° and 64.5° with the crystal planes of (111) and (220), respectively. The narrow shape of the diffraction peak linked to the crystal plane of (002), (101) and (102) suggests the high crystallization and graphitization degree of MWCNTs due to purification. It is important to state the weak diffraction peak of carbon at 51.2° and 75.2°, earlier present on the MWCNTs disappeared due to the suppression of the graphite carbon by the Ag<sup>0</sup> [30]. It is also noteworthy that there was slight decrease on the diffraction peaks of carbon with the deposition of Ag<sup>0</sup> which confirms the result of the EDS in Table 1 that illustrated decrease of carbon content through the incorporation of Ag<sup>0</sup>. The appearance of the graphite carbon and silver nanoparticles at their respective peaks confirms the incorporation of the later into the former. The average crystallite sizes of 19.04 nm were obtained for MWCNTs-Ag<sup>0</sup> using Scherrer equation. It can also be seen in Figure 1b that the XRD spectra of MWCNTs-Ag<sup>0</sup>/PVAc shows the presence of graphite carbon identified at the 2 theta values of 26.6°, 44.4° and 77.5° with a corresponding crystal plane of (002), (101) and (204). In addition, the presence of Ag<sup>0</sup> were indicated by diffraction peak 38.1° and 64.5° corresponding to the crystal planes (111) and (220). Notably, additional peak was observed at 12.8° and 81.6° due to the PVAc incorporation and were attributed to the crystal planes of (001) and (311) [31,32]. The average

crystallite sizes of MWCNTs-Ag<sup>0</sup>/PVAc obtained from Debye-Scherrer equation was 24.3 nm. The observed increase in the crystallite size may be ascribed to the

incorporated materials on the surface matrix of MWCNTs. The crystallite sizes could serve as binding sites for the metal ions adsorption.

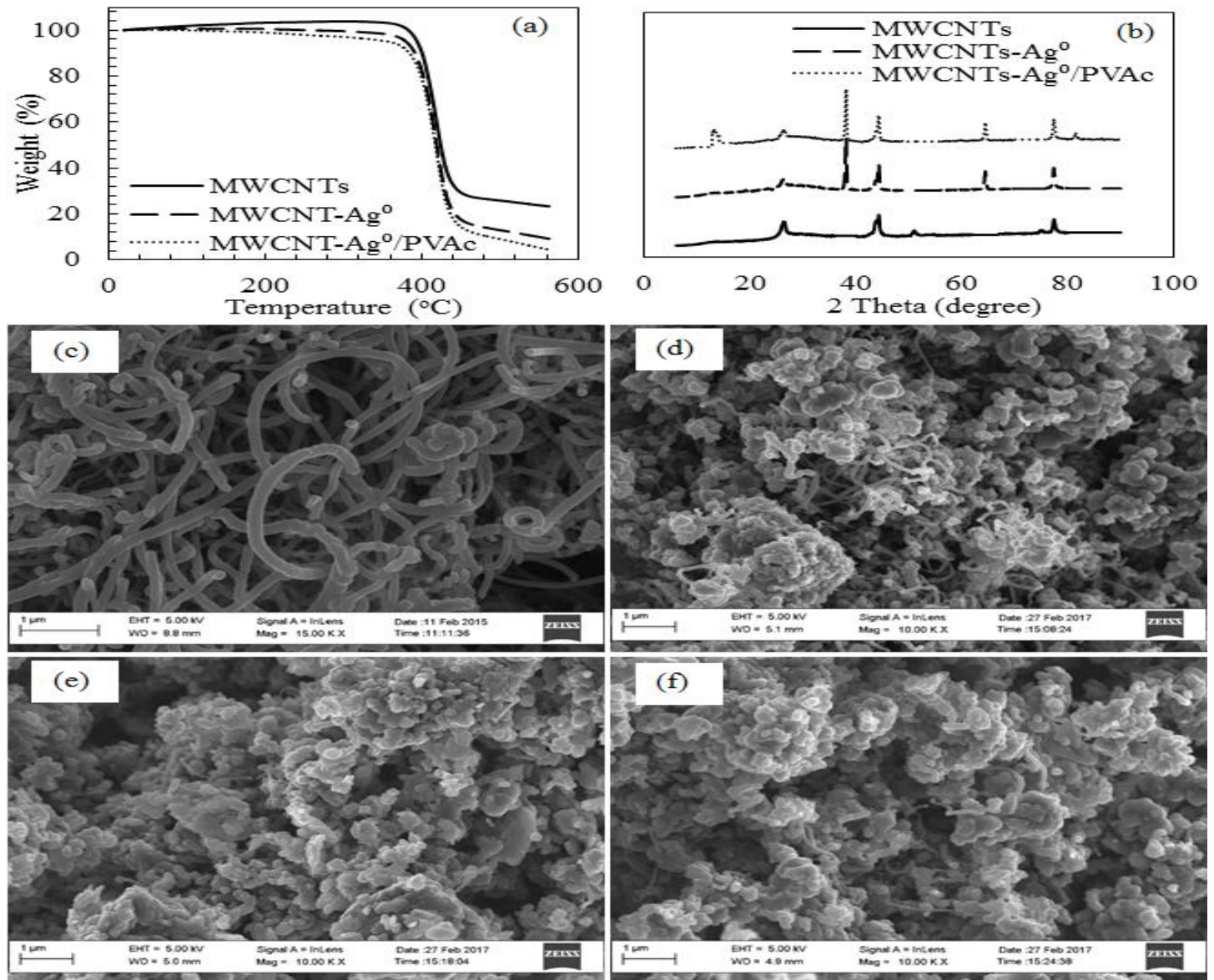


**Figure 1:** (a) TGA of MWCNTs, MWCNTs-Ag<sup>0</sup> and MWCNTs-Ag<sup>0</sup>/PVAc; (b) XRD of MWCNTs, MWCNTs-Ag<sup>0</sup> and MWCNTs-Ag<sup>0</sup>/PVAc; (c) HRSEM image of MWCNTs; (d) HRSEM image of MWCNTs-Ag<sup>0</sup>; (e) HRSEM image of MWCNTs-Ag<sup>0</sup>/PVAc before adsorption and (f) HRSEM image of MWCNTs-Ag<sup>0</sup>/PVAc after adsorption.

The surface morphology of MWCNTs, MWCNTs-Ag<sup>0</sup> and MWCNTs-Ag<sup>0</sup>/PVAc were examined using HRSEM technique and the results presented in Figure 1(c-f). It can be seen from HRSEM image in Figure 1c that MWCNTs has loosely smooth networked cylindrical tubes that were homogeneously distributed and entangled. The morphologies of the MWCNTs observed could be linked to the efficiency of the purification process in the removal of metallic and amorphous impurities. The formation of

smooth cylindrical shapes of the MWCNTs may also be due to the existence of intermolecular forces within the MWCNTs having different sizes of tubular and aggregated structures [33,34]. Typically, the surface morphology of MWCNTs-Ag<sup>0</sup> presented in Figure 1d indicates dense cylindrical shapes of MWCNTs with whitish deposition of Ag<sup>0</sup> on the surface of MWCNTs. The morphology of the MWCNTs-Ag<sup>0</sup> shows the presence of polymorphic shapes that is rocky, spherical and irregular granulated

agglomerates of powder brighter facets of  $\text{Ag}^0$  on the MWCNTs surface fusing loosely with each other at their ends [35]. According to the result presented in Figure 1e, the surface morphology of MWCNTs- $\text{Ag}^0$ /PVAc appears similar, having aggregated morphologies and thick clusters like polymerized beehive structure. The surface morphology and shapes of the MWCNTs- $\text{Ag}^0$ /PVAc indicated the slight suppression of the cylindrical structure of the MWCNTs and the shiny tip presence of the  $\text{Ag}^0$  and PVAc.

The result shows that the materials incorporated on the MWCNTs were appreciably dispersed on the surface. The

suppression of the morphological arrangement of MWCNTs may be linked to the blockage of the inner wall by the  $\text{Ag}^0$  and PVAc particles [36]. Above all, HRSEM analysis was also performed on the MWCNTs- $\text{Ag}^0$ /PVAc after the adsorption studies and the result shown in Figure 1f indicated that the tubular structure of the MWCNTs were retained. The result also revealed slight shortening and breakages of the MWCNTs with the reduction of intermolecular forces within the MWCNTs- $\text{Ag}^0$ /PVAc after the adsorption process because of the uptake of Cr(VI) and Hg(II) onto the surface of the outer walls of the aggregated structure of the MWCNTs- $\text{Ag}^0$ /PVAc [37].

**Table 1:** EDS elemental composition of adsorbents

| Element | MWCNT Atomic (%) | MWCNT- $\text{Ag}^0$ Atomic (%) | MWCNT- $\text{Ag}^0$ /PVAc Atomic (%) |
|---------|------------------|---------------------------------|---------------------------------------|
| C       | 91.8             | 80.6                            | 83.4                                  |
| O       | 6.6              | 5.5                             | 5.0                                   |
| Ag      | 0.0              | 12.6                            | 10.5                                  |
| Fe      | 0.9              | 0.7                             | 0.6                                   |
| Ni      | 0.7              | 0.6                             | 0.5                                   |
| Total   | 100.             | 100                             | 100                                   |

The results of EDS elemental analysis of the MWCNTs, MWCNTs- $\text{Ag}^0$  and MWCNTs- $\text{Ag}^0$ /PVAc are presented in Table 1. It can be seen from the result that the major composition of MWCNTs are 91.8% carbon and 6.6% oxygen. The 0.9% iron and 0.7% nickel were metallic impurities encapsulated within the MWCNTs walls during purification. The result shows the main constituent of MWCNTs- $\text{Ag}^0$  as 80.6% carbon, 5.5% oxygen, 12.6%  $\text{Ag}^0$  and negligible 0.7% and 0.6% of iron and nickel. Overall, the EDS result revealed that MWCNTs- $\text{Ag}^0$ /PVAc were composed of 83.4% carbon, 5.0% oxygen, 10.5%  $\text{Ag}^0$ , 0.6% iron and 0.5% nickel. The noticeable reduction in the carbon content shown in Table 1 could also be attributed to the incorporation of  $\text{Ag}^0$  and PVAc to the MWCNTs [38].

### 3.2 Adsorption of Hg(II) and Cr(VI) by MWCNTs- $\text{Ag}^0$ /PVAc

The preliminary investigation of the adsorption of Hg(II) and Cr(VI) by MWCNTs, MWCNTs- $\text{Ag}^0$  and MWCNTs- $\text{Ag}^0$ /PVAc was conducted and the result revealed a higher adsorption capacity of MWCNTs- $\text{Ag}^0$ /PVAc compared to others. Hence, the influence of pH, adsorption time, adsorbent mass and temperature on the removal of Hg(II) and Cr(VI) by MWCNTs- $\text{Ag}^0$ /PVAc was evaluated to determine the optimal adsorptive conditions.

#### 3.2.1 Influence of pH

The acidic and alkaline nature of the solution is a significant parameter influencing the form of Hg(II) and Cr(VI) contaminants in the solution and the surface charges of the adsorbent [1–3,6]. The influence of pH was investigated in the range 1 to 7 because Hg(II) is unstable in alkaline condition. It can be seen in Figure 2a that the removal of Hg(II) initially increased from pH 1 to 6 and then decreased with further increase in pH to 7. The highest removal of 93.5% was achieved for Hg(II) adsorption by MWCNTs- $\text{Ag}^0$ /PVAc at pH 6. On the other hand, the highest adsorption removal of 82.9% for Cr(VI) was obtained at pH 3, indicating increase in adsorption removal from pH 1 to 3 and decrease beyond pH 3. Generally, Cr(VI) exists in acid solution ( $1 < \text{pH} < 5$ ) as acid chromate ion ( $\text{HCrO}_4^-$ ) and present in large amount with others like  $\text{H}_2\text{CrO}_4$ ,  $\text{Cr}_2\text{O}_7^{2-}$ ,  $\text{Cr}_3\text{O}^{10-}$  and  $\text{Cr}_4\text{O}^{13-}$  [6,39]. Typically, the isoelectric point ( $\text{pH}_{\text{PZC}}$ ) of MWCNTs- $\text{Ag}^0$ /PVAc was evaluated by titration method and obtained as 4.5 whereby the adsorbent was barely charged. Hence, lower removal rates of Hg(II) at  $\text{pH} < \text{pH}_{\text{PZC}}$  may be due to the electrostatic repulsion between positively charged Hg(II) and positively charged adsorbent. The reduction in adsorption effectiveness of Hg(II) at low pH could be attributed to occupation of adsorptive sites of adsorbent by hydrogen ions ( $\text{H}^+$ ) rather than Hg(II), that is competitive adsorption between protons and metal species [1,2]. Comparatively, the adsorption of

Cr(VI) was facilitated and favored at low pH ( $\text{pH} > \text{pH}_{\text{PZC}}$ ) by electrostatic interaction between the negatively charged  $\text{HCrO}_4^-$  (anion) and the positively charged adsorbent [6,39]. Notably, at the  $\text{pH} > \text{pH}_{\text{PZC}}$ , the electrostatic attraction existing between positively charged Hg(II) and negatively charged adsorbent occurred and enhanced the adsorption capacity [3,39]. Above all, increasing the pH decreases the adsorption sites competition between metal

species (Hg(II)) and protons as proposed by the theory of surface complex formation (SCF) [2]. On the contrary, low adsorption of Cr(VI) were revealed at  $\text{pH} > \text{pH}_{\text{PZC}}$  (see Figure 2a) up to the alkaline medium due to competition between  $\text{OH}^-$  and  $\text{Cr}_2\text{O}_7^{2-}$  which is the dominant form of Cr(VI) in the medium [39]. The results of this study corresponds with similar results reported over the literature for Hg(II) and Cr(VI) adsorption [1,6].

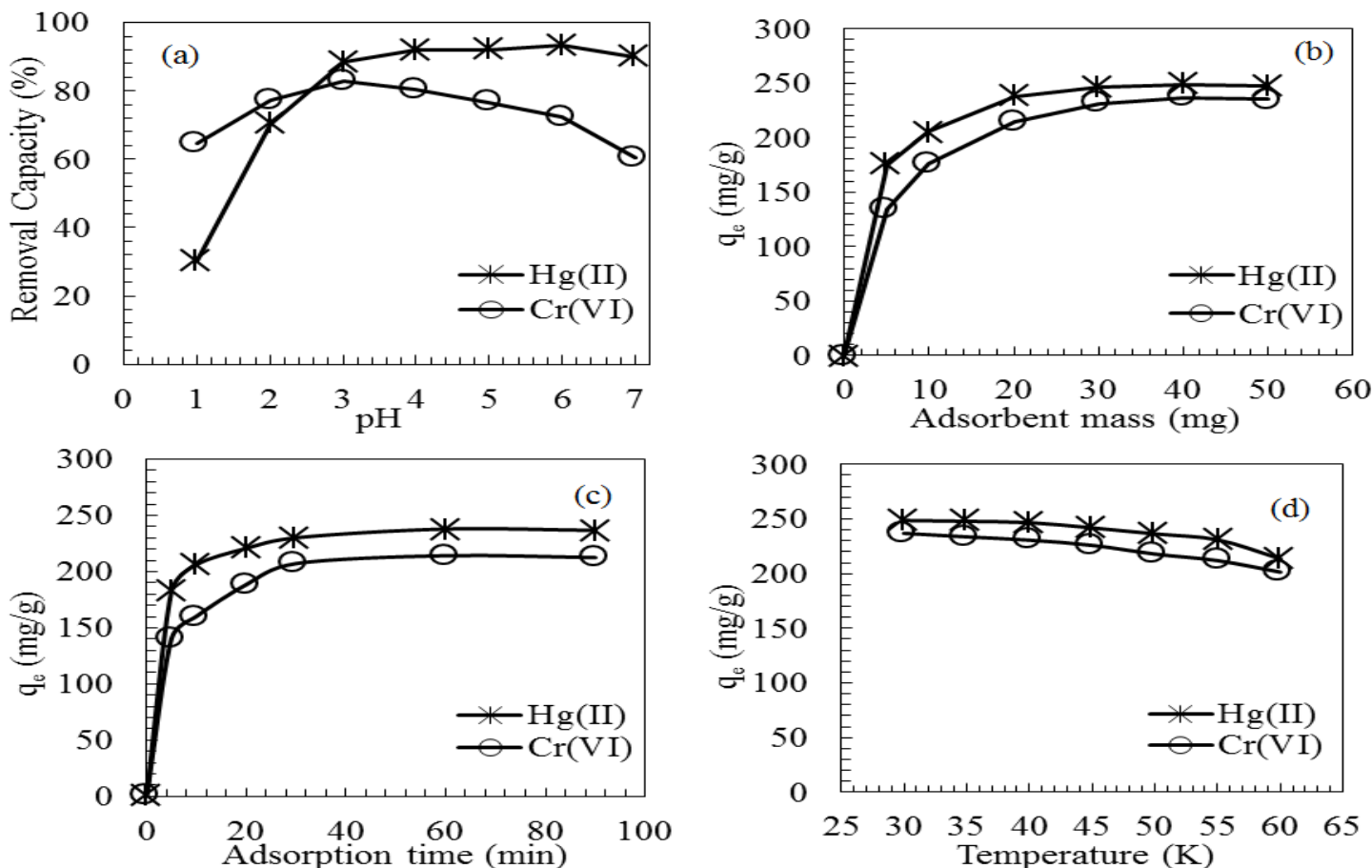


**Figure 2:** Influence of (a) pH; (b) adsorbent mass; (c) adsorption time and (d) temperature on the removal of Hg(II) and Cr(VI) by MWCNTs-Ag<sup>0</sup>/PVAc.

### 3.2.2 Influence of Adsorbent Mass and Adsorption Isotherm

Adsorbent mass had been reported as an important parameter that influences the adsorption of Hg(II) and Cr(VI) [3,39]. As seen in Figure 2b, the adsorption capacity of MWCNTs-Ag<sup>0</sup>/PVAc towards Hg(II) improved from 175 to 249 mg/g, while the adsorption of Cr(VI) increased from 134 to 237 mg/g using the same adsorbent mass of 5 to 40 mg. The observed increment may be linked to the availability of greater adsorption sites [3]. Different from the above trend, the adsorption capacity of Hg(II) and Cr(VI) decreased to 248 and 235 mg/g by increasing the adsorbent mass to 50 mg. This behavior

may be ascribed to the greater occupation of the active sites by smaller masses and possible overlapping of the binding sites by larger masses [39]. Above all, it was observed that more Hg(II) ions were adsorbed at each adsorbent mass compared to Cr(VI) and may be attributed to the differences in the electronegativity of the metal ions. The electronegativities of Hg(II) and Cr(VI) are 2.00 and 1.66, respectively. Thus, metal ion with higher electronegativity tends to adsorb faster, compared with a lower electronegative metal ion.

The adsorption isotherm study is important in the description of the interaction between adsorbents and target pollutants [2]. Typically, three adsorption isotherm

models such as Langmuir, Freundlich and Dubinin-Radushkevich (D-R) were investigated and the obtained parameters presented in Table 2. As shown in Figure 3(a, b) and Table 2, Langmuir isotherm with higher correlation coefficient ( $R^2$ ) of 0.993 and 0.979 for Hg(II) and Cr(VI) revealed a better fitting to experimental data compared to Freundlich and D-R. This indicate that the adsorption of Hg(II) and Cr(VI) by MWCNTs-Ag<sup>0</sup>/PVAc corresponds to monolayer homogenous coverage of the adsorption process.

In addition, the adsorption capacity for the monolayer adsorption process were obtained as 238.10 mg/g and 175.44 mg/g for Hg(II) and Cr(VI), respectively. Also,  $0 < R_L < 1$  obtained in Table 2 is an indication of a good adsorption performance.

### 3.2.3 Influence of adsorption time and adsorption kinetics

Time dependent investigations were performed to evaluate the adsorptive rate of Hg(II) and Cr(VI) ions on the MWCNTs-Ag<sup>0</sup>/PVAc and the result presented in Figure 2c. According to the result, rapid removal of Hg(II) and Cr(VI) were observed within the first 30 min which gradually slowed down until equilibrium was achieved at the adsorption time of 60 min. The observed adsorption trend of the metal ions may be due to the larger adsorption sites availability [3]. Beyond 60 min, the adsorption of the metal ions declined, which could be attributed to the saturation of the binding sites on the adsorbent surface by the metal ions [40]. The adsorption of more Hg(II) ions than Cr(VI) may be linked to the higher electronegativity of the former than the later.

**Table 2:** Isotherm and kinetic parameters of Hg(II) and Cr(VI) adsorption by MWCNTs-Ag<sup>0</sup>/PVAc.

| Models              | Parameters                                      | Hg(II)   | Cr(VI)             |                    |
|---------------------|---|--|--------------------|--------------------|
| Isotherm            | Langmuir  | $q_m$ (mg/g)                                     | 249                | 237                |
|                     |   | $K_L$ (L/min)                                    | 1.50               | 0.26               |
|                     |   | $R_L$  | 0.006              | 0.036              |
|                     |   | $R^2$  | 0.993              | 0.979              |
|                     | Freundlich                                      | $n_F$  | 12.97              | 4.18               |
|                     |   | $K_F$ (mg/g)                                     | 330.14             | 293.17             |
|                     |   | $R^2$  | 0.818              | 0.901              |
|                     | Dubinin-Radushkevich                            | $K_{ad}$   | $3 \times 10^{-9}$ | $2 \times 10^{-6}$ |
|                     |   | $q_s$  | 282.08             | 224.5              |
|                     | Kinetics  | Pseudo-first order                               | $R^2$              | 0.456              |
| $q_{e, cal}$ (mg/g) |   |  | 151.77             | 211.3              |
| Pseudo-second order |   | $K_1$ (1/min)                                    | 0.105              | 0.086              |
|                     |   | $R^2$  | 0.989              | 0.996              |
|                     |   | $q_e$ (mg/g)                                     | 476.19             | 434.78             |
|                     |   | $K_2$ (g mg <sup>-1</sup> min <sup>-1</sup> )    | 0.00130            | 0.0008             |
| Elovich             |   | $R^2$  | 0.9999             | 0.9997             |
|                     |   | $\alpha$ (g mg <sup>-1</sup> min <sup>-2</sup> ) | 576.50             | 784.49             |
|                     | $\beta$ (mg g <sup>-1</sup> min <sup>-1</sup> ) | 0.079  | 0.055              |                    |
|                     | $R^2$   | 0.917  | 0.920              |                    |

To further understand the adsorption performance of MWCNTs-Ag<sup>0</sup>/PVAc for Hg(II) ions than Cr(VI), adsorption kinetic experiments were explored and fitted to kinetic models such as pseudo-first order, pseudo-second order and Elovich model. The results presented in Table 2 and Figure 3c revealed that the  $R^2$  of pseudo-second order of the metal ions were larger (0.9999 for Hg(II) and 0.9994 for Cr(VI)) than that of pseudo-first order (0.989 for Hg(II) and 0.996 for Cr(VI)) and Elovich (0.917 for Hg(II) and

0.920 for Cr(VI)) model indicating a better fit of the experimental data to pseudo-second order. Overall, the adsorption kinetics indicate that the adsorption mechanism of Hg(II) and Cr(VI) ions were controlled by chemical adsorption interaction. In this study, the chemisorption controlled adsorption of Hg(II) and Cr(VI) ion onto MWCNTs-Ag<sup>0</sup>/PVAc involves the generation of valence forces by the exchange and sharing of electrons between the metal ions and the adsorbent [2].

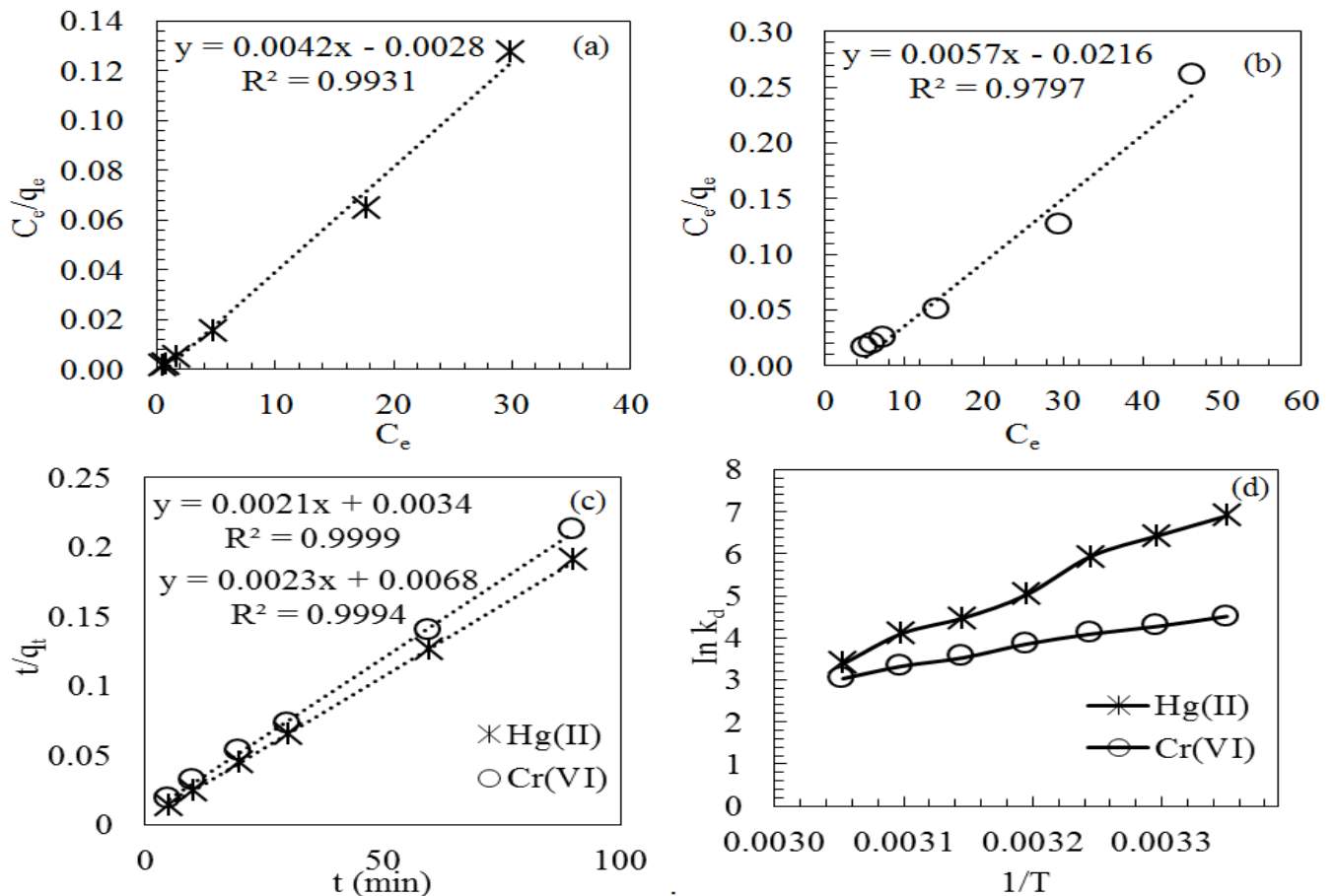


**Figure 3:** (a) Langmuir isotherm of Hg(II) adsorption; (b) Langmuir isotherm of Hg(II) adsorption; (c) Pseudo-second order kinetics of Hg(II) and Cr(VI) adsorption and (d) thermodynamics of metal ions adsorption by MWCNTs-Ag<sup>0</sup>/PVAc

3.2.4 Influence of temperature and thermodynamics

The influence of temperature on the adsorption capacity of MWCNTs-Ag<sup>0</sup>/PVAc for Hg(II) and Cr(VI) was investigated and the result shown in Figure 2d. Importantly, increase in temperature from 30 to 60 °C

resulted to decline in the adsorption of metal ions on the adsorbent surface from 249 to 214 mg/g for Hg(II) and from 237 to 202 mg/g for Cr(VI) ion. The Van't Hoff relationship plot and evaluated thermodynamic parameters are shown in Figure 3d and Table 3, respectively.

**Table 3:** Thermodynamic parameters for the removal of Hg(II) and Cr(VI) by MWCNTs-Ag<sup>0</sup>/PVAc

| Temperature (°C) | Hg(II)       |              |              | Cr(VI)       |              |              |
|------------------|--------------|--------------|--------------|--------------|--------------|--------------|
|                  | $\Delta G^0$ | $\Delta H^0$ | $\Delta S^0$ | $\Delta G^0$ | $\Delta H^0$ | $\Delta S^0$ |
| 30               | -17389       | -99859       | -271         | -11368       | -41259       | -98          |
| 35               | -16465       |              |              | -10949       |              |              |
| 40               | -15455       |              |              | -10652       |              |              |
| 45               | -13269       |              |              | -10184       |              |              |
| 50               | -12011       |              |              | -9475        |              |              |
| 55               | -11201       |              |              | -9077        |              |              |
| 60               | -9368        |              |              | -8399        |              |              |

Accordingly, the  $\Delta G^0$  were all negative for both Hg(II) and Cr(VI) at the various temperatures, indicating that the adsorption process of the metal ions were spontaneous on the surface of MWCNTs-Ag<sup>0</sup>/PVAc. The

negative values of  $\Delta H^0$  suggests that the adsorption procedure of Hg(II) and Cr(VI) releases heat (exothermic process), an indication that increase in temperature did not facilitate the adsorption process. In the end, the negative

value of  $\Delta S^\circ$  for both Hg(II) and Cr(VI) is indicative of reduction in the stoichiometry of randomness at the adsorbent/adsorbate interface.

#### 4 CONCLUSION

In this study, MWCNTs-Ag<sup>0</sup>/PVAc was successfully fabricated by the effective incorporation of highly dispersed Ag<sup>0</sup> and PVAc on the surface of MWCNTs for the removal of Hg(II) and Cr(VI) ions from wastewater. Improved Hg(II) and Cr(VI) removal performance was achieved at the optimum pH (6 for Hg(II) and 3 for Cr(VI)), adsorbent mass (40 mg), adsorption time (60 min) and temperature (30 °C). The experimental data fitted better to the Langmuir isotherm, compared to Freundlich and D-R isotherm models. The maximum adsorption capacity of Hg(II) and Cr(VI) adsorption onto MWCNTs-Ag<sup>0</sup>/PVAc for the monolayer coverage were 249 mg/g and 237 mg/g, respectively. Equally, the kinetic data showed best suitability to pseudo-second order model for the kinetic mechanism explanation, indicating chemisorption-controlled adsorption process. MWCNTs-Ag<sup>0</sup>/PVAc showed optimum performance effectiveness to remove Hg(II) and Cr(VI) from wastewater than other nanoadsorbents..

#### REFERENCES

- [1] Pei, P. Xu, Y. Wang, L. Liang, X. Sun, Y. "Thiol-functionalized montmorillonite prepared by one-step mechanochemical grafting and its adsorption performance for mercury and methylmercury", *Sci. Total Environ.* 806, 2022, pp.150510. <https://doi.org/10.1016/j.scitotenv.2021.150510>.
- [2] Long, C. Li, X. Jiang, Z. Zhang, P. Qing, Z. Qing, T. Feng, B. "Adsorption-improved MoSe<sub>2</sub> nanosheet by heteroatom doping and its application for simultaneous detection and removal of mercury (II)", *J. Hazard. Mater.* 413, 2021, pp.125470. <https://doi.org/10.1016/j.jhazmat.2021.125470>.
- [3] Chen, C. Chen, Z. Shen, J. Kang, J. Zhao, S. Wang, B. Chen, Q. Li, X. "Dynamic adsorption models and artificial neural network prediction of mercury adsorption by a dendrimer-grafted polyacrylonitrile fiber in fixed-bed column", *J. Clean. Prod.* 310, 2021, pp.127511. <https://doi.org/10.1016/j.jclepro.2021.127511>.
- [4] Selimin, M.A. Latif, A.F.A. Lee, C.W. Muhamad, M.S. Basri, H. Lee, T.C. "Adsorption efficiency of hydroxyapatite synthesised from black tilapia fish scales for chromium (VI) removal", *Mater. Today Proc.* (2021). <https://doi.org/10.1016/j.matpr.2021.10.008>.
- [5] Egbosiuba, T.C., Abdulkareem, A.S., Kovo, A.S., Afolabi, E.A., Tijani, J.O., Bankole, M.T., Bo, S. and Roos, W.D. "Adsorption of Cr (VI), Ni (II), Fe (II) and Cd (II) ions by KIAgNPs decorated MWCNTs in a batch and fixed bed process". *Scientific reports*, 11(1), 2021, pp.1-20. <https://doi.org/10.1038/s41598-020-79857-z>.
- [6] Yang, H.R., Li, S.S., Shan, X.C., Yang, C., An, Q.D., Zhai, S.R. and Xiao, Z.Y., "Hollow polyethyleneimine/carboxymethyl cellulose beads with abundant and accessible sorption sites for ultra-efficient chromium (VI) and phosphate removal". *Separation and Purification Technology*, 278, 2021, pp.119607. <https://doi.org/10.1016/j.seppur.2021.119607>.
- [7] WHO, Guidelines for Drinking-water Quality, Fourth Ed. (2017) 631. [https://doi.org/10.1016/S1462-0758\(00\)00006-6](https://doi.org/10.1016/S1462-0758(00)00006-6).
- [8] Sun, Y., Zhou, S., Pan, S.Y., Zhu, S., Yu, Y. and Zheng, H., "Performance evaluation and optimization of flocculation process for removing heavy metal". *Chemical Engineering Journal*, 385, 2020, pp.123911. <https://doi.org/10.1016/j.cej.2019.123911>.
- [9] Maslova, M., Ivanenko, V., Yanicheva, N. and Gerasimova, L., "The effect of heavy metal ions hydration on their sorption by a mesoporous titanium phosphate ion-exchanger". *Journal of Water Process Engineering*, 35, 2020, pp.101233. <https://doi.org/10.1016/j.jwpe.2020.101233>.
- [10] Chen, Q., Yao, Y., Li, X., Lu, J., Zhou, J. and Huang, Z., "Comparison of heavy metal removals from aqueous solutions by chemical precipitation and characteristics of precipitates". *Journal of water process engineering*, 26, 2018, pp.289-300. <https://doi.org/10.1016/j.jwpe.2018.11.003>.
- [11] Tijani, J.O., Abdullahi, M.N., Bankole, M.T., Mustapha, S., Egbosiuba, T.C., Ndamitso, M.M., Abdulkareem, A.S. and Muzenda, E., "Photocatalytic and toxicity evaluation of local dyeing wastewater by aluminium/boron doped WO<sub>3</sub> nanoparticles". *Journal of Water Process Engineering*, 44, 2021, pp.102376. <https://doi.org/10.1016/j.jwpe.2021.102376>.
- [12] Egbosiuba, T.C., Abdulkareem, A.S., Kovo, A.S., Afolabi, E.A., Tijani, J.O. and Roos, W.D., "Enhanced adsorption of As (V) and Mn (VII) from industrial wastewater using multi-walled carbon nanotubes and carboxylated multi-walled carbon nanotubes". *Chemosphere*, 254, 2020, pp.126780. <https://doi.org/10.1016/j.chemosphere.2020.126780>.

- [13] Igwegbe, C.A. Onukwuli, O.D. Ighalo, J.O. Okoye, P.U. "Adsorption of Cationic Dyes on *Dacryodes edulis* Seeds Activated Carbon Modified Using Phosphoric Acid and Sodium Chloride", *Environ. Process.* 7, 2020, pp.1151–1171. <https://doi.org/10.1007/s40710-020-00467-y>.
- [14] Mustapha, S., Tijani, J.O., Ndamitso, M.M., Abdulkareem, S.A., Shuaib, D.T., Mohammed, A.K. and Sumaila, A., "The role of kaolin and kaolin/ZnO nanoadsorbents in adsorption studies for tannery wastewater treatment". *Scientific Reports*, 10(1), 2020, pp.1-22. <https://doi.org/10.1038/s41598-020-69808-z>.
- [15] Hamzat, W.A., Abdulkareem, A.S., Bankole, M.T., Tijani, J.O., Kovo, A.S. and Abubakre, O.K., "Adsorption studies on the treatment of battery wastewater by purified carbon nanotubes (P-CNTs) and polyethylene glycol carbon nanotubes (PEG-CNTs)". *Journal of Environmental Science and Health, Part A*, 54(9), 2019, pp.827-839. <https://doi.org/10.1080/10934529.2019.1596701>.
- [16] Egbosiuba, T.C. Abdulkareem, A.S. "Highly efficient as-synthesized and oxidized multi-walled carbon nanotubes for copper(II) and zinc(II) ion adsorption in a batch and fixed-bed process", *J. Mater. Res. Technol.* 2021. <https://doi.org/10.1016/j.jmrt.2021.09.094>.
- [17] Egbosiuba, T.C., Egwunyenga, M.C., Tijani, J.O., Mustapha, S., Abdulkareem, A.S., Kovo, A.S., Krikstolaityte, V., Veksha, A., Wagner, M. and Lisak, G., "Activated multi-walled carbon nanotubes decorated with zero valent nickel nanoparticles for arsenic, cadmium and lead adsorption from wastewater in a batch and continuous flow modes". *Journal of Hazardous Materials*, 423, 2022. pp.126993. <https://doi.org/10.1016/j.jhazmat.2021.126993>.
- [18] Mustapha, S., Tijani, J.O., Ndamitso, M.M., Abdulkareem, A.S., Shuaib, D.T. and Mohammed, A.K., "Adsorptive removal of pollutants from industrial wastewater using mesoporous kaolin and kaolin/TiO<sub>2</sub> nanoadsorbents". *Environmental Nanotechnology, Monitoring & Management*, 15, 2021. p.100414. <https://doi.org/10.1016/j.enmm.2020.100414>.
- [19] Ogarekpe, N.M., Tenebe, I.T., Emenike, P.C., Antigha, R.E., Basse, I.E., Attah, I.C. and Ekeng, E.E., "Preliminary investigation on the use of *Moringa oleifera* for the purification of lead polluted wastewater". *Nigerian Journal of Technology*, 38(1), 2019, pp.253-257. <https://doi.org/10.4314/njt.v38i1.30>.
- [20] Agarry, S.E. Owabor, C.N. "Evaluation of the adsorption potential of rubber (*Hevea brasiliensis*) seed pericarp-activated carbon in abattoir wastewater treatment and in the removal of iron (III) ions from aqueous solution", *Niger. J. Technol.* 31, 2012, pp. 346–358.
- [21] Ohimor, E.O. Temisa, D.O. Ononiwu, P.I. "Production of Activated Carbon from Carbonaceous Agricultural Waste Material: Coconut Fibres", *Niger. J. Technol.* 40, 2021, pp. 19–24. <https://doi.org/10.4314/njt.v40i1.4>.
- [22] Oribayo, O. Olaleye, O.O. Akinyanju, A.S. Omolaja, K.O. Williams, S.O. "Coconut shell-based activated carbon as adsorbent for the removal of dye from aqueous solution: equilibrium, kinetics, and thermodynamic studies", *Niger. J. Technol.* 39, 2021 1076–1084. <https://doi.org/10.4314/njt.v39i4.14>.
- [23] Egbosiuba, T.C., Abdulkareem, A.S., Kovo, A.S., Afolabi, E.A., Tijani, J.O., Auta, M. and Roos, W.D., "Ultrasonic enhanced adsorption of methylene blue onto the optimized surface area of activated carbon: Adsorption isotherm, kinetics and thermodynamics". *Chemical engineering research and design*, 153, 2020, pp.315-336. <https://doi.org/10.1016/j.cherd.2019.10.016>.
- [24] Bankole, M.T., Mohammed, I.A., Abdulkareem, A.S., Tijani, J.O., Ochigbo, S.S., Abubakre, O.K. and Afolabi, A.S., "Optimization of supported bimetallic (Fe-Co/CaCO<sub>3</sub>) catalyst synthesis parameters for carbon nanotubes growth using factorial experimental design". *Journal of Alloys and compounds*, 749, 2018, pp.85-102. <https://doi.org/10.1016/j.jallcom.2018.03.150>.
- [25] Bhaumik, M. Maity, A. Brink, H.G. "Zero valent nickel nanoparticles decorated polyaniline nanotubes for the efficient removal of Pb(II) from aqueous solution: Synthesis, characterization and mechanism investigation", *Chem. Eng. J.* 417, 2021, pp.127910. <https://doi.org/10.1016/j.cej.2020.127910>.
- [26] Al Hamouz, O.C.S., Adelabu, I.O. and Saleh, T.A., "Novel cross-linked melamine based polyamine/CNT composites for lead ions removal". *Journal of environmental management*, 192, 2017, pp.163-170. <https://doi.org/10.1016/j.jenvman.2017.01.056>.
- [27] Egbosiuba, T.C., Abdulkareem, A.S., Tijani, J.O., Ani, J.I., Krikstolaityte, V., Srinivasan, M., Veksha, A. and Lisak, G., "Taguchi optimization design of diameter-controlled synthesis of multi walled carbon nanotubes for the adsorption of Pb (II) and Ni (II) from chemical industry

- wastewater". *Chemosphere*, 266, 2021, pp.128937. <https://doi.org/10.1016/j.chemosphere.2020.128937>.
- [28] Sarkar, S., Tiwari, N., Basu, A., Behera, M., Das, B., Chakraborty, S., Sanjay, K., Suar, M., Adhya, T.K., Banerjee, S. and Tripathy, S.K., "Sorptive removal of malachite green from aqueous solution by magnetite/coir pith supported sodium alginate beads: Kinetics, isotherms, thermodynamics and parametric optimization". *Environmental Technology & Innovation*, 24, 2021, pp.101818. <https://doi.org/10.1016/j.eti.2021.101818>.
- [29] Sangeetha, K. Vidhya, G. Girija, E.K. "Lead and cadmium removal from single and binary metal ion solution by novel hydroxyapatite/alginate/gelatin nanocomposites", *J. Environ. Chem. Eng.* 2018. <https://doi.org/10.1016/j.jece.2018.01.018>.
- [30] Cheng, Y., Li, H., Fang, C., Ai, L., Chen, J., Su, J., Zhang, Q. and Fu, Q., "Facile synthesis of reduced graphene oxide/silver nanoparticles composites and their application for detecting heavy metal ions". *Journal of Alloys and Compounds*, 787, 2019, pp.683-693. <https://doi.org/10.1016/j.jallcom.2019.01.320>.
- [31] Abdelghany, A.M., Meikhaail, M.S. and Asker, N., "Synthesis and structural-biological correlation of PVC/PVAc polymer blends". *Journal of Materials Research and Technology*, 8(5), 2019, pp.3908-3916. <https://doi.org/10.1016/j.jmrt.2019.06.053>.
- [32] Taghiyari, H.R., Majidi, R., Armaki, S.M.M. and Haghghatparast, M., "Graphene as reinforcing filler in polyvinyl acetate resin". *International Journal of Adhesion and Adhesives*, 2021. pp.103075. <https://doi.org/10.1016/j.ijadhadh.2021.103075>.
- [33] Oyewemi, A., Abdulkareem, A.S., Tijani, J.O., Bankole, M.T., Abubakre, O.K., Afolabi, A.S. and Roos, W.D., Controlled syntheses of multi-walled carbon nanotubes from bimetallic Fe–Co catalyst supported on kaolin by chemical vapour deposition method. *Arabian Journal for Science and Engineering*, 44(6), 2019, pp.5411-5432. <https://doi.org/10.1007/s13369-018-03696-4>.
- [34] Bankole, M.T., Abdulkareem, A.S., Mohammed, I.A., Ochigbo, S.S., Tijani, J.O., Abubakre, O.K. and Roos, W.D., "Selected heavy metals removal from electroplating wastewater by purified and polyhydroxylbutyrate functionalized carbon nanotubes adsorbents". *Scientific reports*, 9(1), 2019, pp.1-19. <https://doi.org/10.1038/s41598-018-37899-4>.
- [35] Iqbal, A. Saeed, A. Kausar, A. Arshad, M. Mahar, J. "Synthesis and characterization of DGEBA composites reinforced with Cu/Ag modified carbon nanotubes", *Heliyon*. 5, 2019, pp.e01733. <https://doi.org/10.1016/j.heliyon.2019.e01733>.
- [36] Aqel, A. El-Nour, K.M.M.A. Ammar, R.A.A. Al-Warthan, A. "Carbon nanotubes, science and technology part (I) structure, synthesis and characterisation", *Arab. J. Chem.* 5, 2012, pp.1–23. <https://doi.org/10.1016/j.arabjc.2010.08.022>.
- [37] Bankole, M.T., Abdulkareem, A.S., Tijani, J.O., Ochigbo, S.S., Afolabi, A.S. and Roos, W.D., "Chemical oxygen demand removal from electroplating wastewater by purified and polymer functionalized carbon nanotubes adsorbents". *Water Resources and Industry*, 18, 2017, pp.33-50. <https://doi.org/10.1016/j.wri.2017.07.001>.
- [38] Barabás, R., Katona, G., Bogya, E.S., Diudea, M.V., Szentes, A., Zsirka, B., Kovács, J., Kékedy-Nagy, L. and Czíkó, M., Preparation and characterization of carboxyl functionalized multiwall carbon nanotubes–hydroxyapatite composites. *Ceramics International*, 41(10), 2015, pp.12717-12727. <https://doi.org/10.1016/j.ceramint.2015.06.104>.
- [39] Almeida, A.C.M., do Nascimento, R.A., Amador, I.C.B., de Sousa Santos, T.C., Martelli, M.C., de Faria, L.J.G. and da Paixão Ribeiro, N.F. Chemically activated red mud: assessing structural modifications and optimizing adsorption properties for hexavalent chromium. *Colloids and Surfaces A: Physicochemical and Engineering Aspects*, 628, 2021, pp.127325. <https://doi.org/10.1016/j.colsurfa.2021.127325>.
- [40] Filipowiak, K., Wieszczycka, K., Buchwald, T., Nowicki, M., Wójcik, G., Aksamitowski, P. and Staszak, K., "Reduction-adsorption of chromium (VI) by using IL-imprinted resin-innovative solution for water purification". *Journal of Molecular Liquids*, 343, 2021, p.116977. <https://doi.org/10.1016/j.molliq.2021.116977>.